MULTI-OBJECTIVE OPTIMIZATION BY SIMULATED ANNEALING APPLIED TO IMAGE RECONSTRUCTION BY ELECTRICAL IMPEDANCE TOMOGRAPHY

Amanda Vieira Fernandes
Marcos de Sales Guerra Tsuzuki
Thiago de Castro Martins
Polytechnic School of University of São Paulo, Av. Prof. Luciano Gualberto, Travessa 3, n° 380, Butantã São Paulo, 05508-010
amanda.vieira.fernandes@usp.br
thiago@usp.br

Abstract. *The image reconstruction from the Electrical Impedance Tomography (EIT) can be approached as an optimization problem, in which is desired to minimize the Euclidean distance between the potential values measured in the cross section of the body and the calculated values, for every pattern of current applied, through the modelling of the problem by the Finite Elements Method (FEM). It's known, a priori, that this formulation is ill-posed, which increases dependence of the EIT to the reconstruction algorithm, which must has any regularization technique to improve the conditioning of the problem. Therefore, this project proposes the use of an Multi-Objective Optimization algorithm in order to find the set of optimal solutions to the problem, aiming the minimization both the Euclidean distance and a regularization parameter.*

Keywords: *electrical impedance tomography, multi-objective optimization, simulated annealing, regularization techniques.*

1. INTRODUCTION

Since the early 80s, a new tomographic technique is being developed: the Electrical Impedance Tomography (EIT). It consists on the non-invasive obtainment of images of the cross section of a solid body based on the estimative of the electrical conductivity (or resistivity) distribution inside a domain (Henderson and Webster, 1978; Price, 1979; Barber and Brown, 1984). Its most common use is in monitoring and medical diagnostics (Barber and Brown, 1984). In particular, imaging of lung stands out due to its size and high resistivity contrasts, features that make the image estimation using this technique easier (Frerichs, 2000).

EIT image reconstruction is often approached as a problem of non-linear non-convex optimization. Under this approach, the problem is converted in the problem of minimizing the difference between physical measures and simulations of a parametrized model (Herrera, 2007; Mello *et al.*, 2008; Martins *et al.*, 2012). As the underlying optimization problem is often ill-conditioned, additional regularization terms are added to its objective function in order to stabilize the solution (Vauhkonen *et al.*, 1998). The *a priori* determination of the *weight* of the regularizing terms is often difficult. In this context, multi-objective optimization arises as a promising technique, allowing for the determination of a family of possible solutions with different balances between the regularizing terms and the original objective.

2. ELECTRICAL IMPEDANCE TOMOGRAPHY

Imaging techniques are able to obtain images of the cross section of a solid body through the association between the information(obtained by a series of measures in different directions of the section analyzed) and a computer which, once coupled to the *hardware* used to obtain these data, reconstructs the image according to a predetermined mathematical algorithm (Bates *et al.*, 1983).
The Electrical Impedance Tomography (EIT) is presented as an alternative technique to the traditional tomography, since the algorithms that have been developed use the information coming from the voltage values measured by electrodes placed around the section analyzed to reconstruct its internal image. The reconstructions obtained by this method have a low resolution when compared to other techniques. However, even not showing resolution results as satisfactory as other techniques, the EIT method stands out, as its tomograph doesn't expose the body region in analysis to any kind of radiation, is portable and low cost, making feasible its clinical application Cheney *et al.* (1990); Browne (2001).
The mathematical approach used to solve the estimation problem can be sectioned in two parts: the resolution of the *direct problem*, which consists in modeling the electrical potentials from an explicit conductivity function (our resistivity) of the domain; and the resolution of the *inverse problem*, which consists in calculating the conductivity(or resistivity) distribution inside de domain using the voltage values measured in the surroundings of the section (Murai and Kagawa, 1985; Kallman and Berryman, 1992). It is known, in advance, that the inverse problem is ill-posed (Sylvester and Uhlmann, 1987; Glisser *et al.*, 1990), increasing the dependency of the EIT reconstruction to the algorithm used, which must pos-

sess some *regularization technique* to improve the conditioning of the problem (Tikhonov, 1991; Adler and Guardo, 1996; West *et al.*, 2001).

2.1 Formulation of the Finite Elements Method

The electrical current flow, under a quasi-static approximation, is described by the following elliptic equation:

$$\nabla \left(\sigma \nabla \phi \right) = 0 \tag{1}$$

where σ is the film conductivity and ϕ is the electrical potential. The typical *forward problem* in EIT is given the conductivity distribution σ and the current J injected through boundary electrodes, find the potential distribution ϕ within Ω and in particular the resulting potentials at the measurement electrodes ϕ_m. At the boundary, currents are injected through electrodes; thus the current density J_l injected through the l-th electrode is given by (current pattern)

$$\sigma \frac{\partial \phi}{\partial \hat{n}} = J_l \tag{2}$$

and the current density is zero elsewhere at the boundary Brown and Seagar (1987).

The exact analytical solutions to the Eq. (1) aren't well known. One way to obtain approximate solutions is the Finite Elements Method (FEM) Herrera (2007). The method consists in decomposing the domain into discrete elements and seek a solution $\tilde{\phi}$ using a linear approximation to the potential function ϕ. Applying continuity conditions and defining a global total error metric to be minimized, it is possible to convert the Eq. (1) into a linear system:

$$\mathbf{K}(\sigma)\mathbf{\Phi} = \mathbf{C} \tag{3}$$

Where: $\mathbf{K}(\sigma) \in \mathbb{R}^{s \times s}$ is the Conductivity Matrix related to a particular conductance distribution σ_p; $\mathbf{\Phi}$ is a vector of nodal potentials; $\mathbf{C}$ is a vector of nodal currents (null for all nodes, except the electrodes); and s is the number of nodes in the system.

3. THE INVERSE PROBLEM AS AN OPTIMIZATION PROBLEM

The EIT's inverse problem consists in, given the domain Ω, the current $\boldsymbol{J}$ injected into the electrodes and the potential ϕ_m in the electrodes, determining the conductivity distribution σ.

Once there are known efficient methods (as the FEM described above) to solve de direct problem, it is possible to approach the inverse problem as an optimization problem, in which the variables are a parameterization of the conductivity in the domain (for example, segmenting the domain in intervals of constant conductivity and assigning a parameter to each conductivity values) and the function to be optimized is a measure of how much the solution of the direct problem (calculated from the conductivity produced by the optimization variables) corresponds to the observed data.

Thus, a possible objective function is the Euclidean Distance $E(\sigma)$ between the values of the potentials (ϕ_m^i) measured on the contour and calculated values ($\phi_c^i(\sigma)$) to all current standards applied.

We have, then, the objective function given by:

$$E(\sigma) = \sqrt{\sum_i \left| \phi_m^i - \phi_c^i(\sigma) \right|^2} \tag{4}$$

As stated above, the values of $\phi_c^i(\sigma)$ can be calculated by the FEM by solving the linear systems as in a Eq. (3) for each pattern of current applied, and taking the potentials at the electrodes as $\phi_c^i(\sigma)$ (the values of the potentials internal to the domain can be neglected).

It has been appointed by Mello *et al.* (2008) that the solution of this optimization problem through gradient methods, such as the sequential linear programming used, is inherently difficult since the original problem is ill-posed, which leads to uncertainties in the calculation of the objective function. These are naturally amplified in the calculation of the gradients. In this context, the Simulated Annealing (Herrera, 2007) applied to EIT becomes interesting, because it doesn't require evaluation of derivatives of the objective function.

4. SIMULATED ANNEALING

The Simulated Annealing (SA) (Kirkpatrick *et al.*, 1983) is the heuristic probabilistic method chosen to deal with the EIT problem, once it has the ability to escape from local minimums which frequently occur in this problem.

The technique is based on an algorithm that simulates the process of recrystallization in metal atoms during the annealing. The term "annealing" refers to the thermal cooling that begins with the liquefaction of a crystal at high temperature,

followed by a slow and gradual reduction until the solidification point is reached, at which time the system reaches a "minimum energy" state. Thus, the atoms migrate naturally to positions that minimize the total energy of the system, even if they have to go through high-energy intermediate settings.

The SA combines de advantages of interactive improvement techniques with randomization techniques, resulting in a powerful tool for optimization, which has been used in several problems.

A way to apply the Simulated Annealing to the image reconstruction of Electrical Impedance Tomography is to use the suggested in section 3. formulate the EIT inverse problem as an optimization problem and solve it.

5. MULTI-OBJECTIVE OPTIMIZATION

The term "optimization" refers to the process of finding the best solution to a problem, given a number of constraints relating to it. Considering a situation in which you want to analyze only one single objective, the optimization longs to find the best available solution (called global optimum), or at least a good approximation of the same (Coello, 2006). It is called "mono-objective optimization" the optimization process in which you want to solve only one objective function. In this context, it appears that the Simulated Annealing can be applied to this category due to its characteristics of escaping from local minima, tending to find the global optimum (or near-global).

However, most of the real problems, especially those aimed to the development of engineering models, are placed in order to satisfy more than one objective function, usually conflicting (Suppapitnarm *et al.*, 2000). In this case, there is no single solution that satisfies all objectives simultaneously (Jones *et al.*, 2002). This optimization category is called "multi-objective optimization".

5.1 Resolution of Multi-Objective Problems

The multi-objective optimization can be formally established according to the following formulation (Bandyopadhyay *et al.*, 2008): Find the vector $\overline{x}^* = [x_1^*, x_2^*, ..., x_n^*]^T$ of decision variables that optimizes simultaneously the M objective values $\{f_1(\overline{x}), f_2(\overline{x}), ..., f_M(\overline{x})\}$, while satisfying the constraints, if any.

There are several ways to solve multi-objective problems. Traditionally, their solution is the conversion of all objectives in one single objective function. From this point, we seek to find the solution that maximizes or minimizes it, while maintaining the physical constraints of the system (or process). Thus, the optimization problem results in one single value, reflecting the harmony among all objectives. The problem with this solution is to find a formulation that can transmit the desired harmony to the function ((Ngatchou *et al.*, 2005)).

The conversion of multiple objectives into one single-objective function is usually done by aggregating all functions in a weighted function, or simply choosing one of the objectives and transforming all other ones in restrictions. However, this approach has serious limitations. The first is the need of knowing *a priori* the relative importance of each objective, as well as the limits of those that are converted into constraints. We also emphasize that this aggregation, in both formulations above, generate only one solution. In addition, there is the difficulty in evaluating the compromise among the objectives. Finally, there's a risk of not reaching any solution if the search space isn't convex ((Ngatchou *et al.*, 2005)).

More recently, the use of meta-heuristics became an option quickly accepted by researchers from different disciplines ((Coello, 2006)). Its increasing popularity is mainly due to its ability to find multiple solutions in a single run, work without derivatives, converge quickly to the Pareto optimal solutions with a high accuracy level, deal with combinatorial problems and easy discontinuity of functions (Ngatchou *et al.* (2005)).

In this context, it's necessary to define another important concept: Pareto dominance. In a maximization problem, it's said that a solution $\vec{x_i}$ dominates $\vec{x_j}$ if $\forall k \in 1, 2, ..., M, f_k(\vec{x_i}) \geq f_k(\vec{x_j})$ and $\exists k \in 1, 2, ..., M$, such that $f_k(\vec{x_i}) > f_k(\vec{x_j})$ ((Suppapitnarm *et al.*, 2000)). Thus, the Pareto dominance is used to compare and classify the decision vectors, where $\vec{x_i}$ dominate $\vec{x_j}$ in the Pareto sense means that $F(\vec{x_i})$ is better than $F(\vec{x_j})$ for all objectives, and that there is at least one objective for which $F(\vec{x_i})$ is strictly better than $F(\vec{x_j})$ ((Ngatchou *et al.*, 2005)).

A solution $\vec{y}$ is considered a Pareto optimal if and only if there is no other solution that dominates it. In other words, the solution $\vec{y}$ can't be improved in an objective without at least one of the other objectives is adversely affected. The corresponding objective vector $F(\vec{y})$ is called dominant Pareto vector, or non-inferior, or non-dominated. The set of Pareto optimal solutions is called the Pareto optimal set. The corresponding objective vectors are meant to be the Pareto front (Ngatchou *et al.*, 2005). Figure (1) shows a representation of the Pareto front in a bi-objective problem which we want to minimize f_1 and f_2.
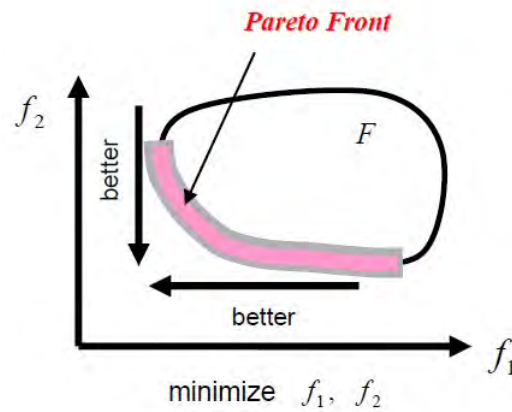
Figure 1: Pareto Front to a Bi-objective Minimization Problem. Adapted from (Ngatchou *et al.*, 2005)

5.2 Multi-Objective Optimization Algorithms by Simulated Annealing

An area of meta-heuristics widely explored by researchers is the algorithms based on Simulated Annealing. There are several different formulations that use the SA to find the Pareto optimal.

As a pioneer in this area, the algorithm Multi-Objective Simulated Annealing (MOSA) developed by Engrand (1997)can be mentioned. In this algorithm, a "composition" of the objective function G is created between each objective and is defined as:

$$G = \sum_{i=1}^{M} ln f_i \tag{5}$$

Where $f_1, ..., f_M$ are M objectives to be minimized. At each iteration, n, the values of $f_1, ..., f_M$ are calculated from values of control variables stored in $\underline{X}_n$, and then replaced in Eq. (5) to produce $G(\underline{X}_n)$. Random perturbations are then applied to each element of $\underline{X}_n$ to obtain $\underline{X}_{n+1}$, for which $G(\underline{X}_{n+1})$ is calculated. As the mono-optimization, the acceptance criteria with the following probability P (calculated using Eq. (6) is then applied between successive operations.

$$P = e^{\left(\frac{-(G(\underline{X}_{n+1}) - G(\underline{X}_n))}{T}\right)} \tag{6}$$

During the course, an archive of non-dominated solutions is maintained. All accepted solutions are candidates for archiving: if a candidate solution dominates any member of the archive, those members are removed and the new solution is added; if the new solution is dominated by any member of the archive, it isn't archived; if the solution doesn't dominate anyone nor is dominated by any member of the file, it's added to it. This technique is outlined in Fig. (2), which shows a minimization bi-objective problem.

However, some aspects of this algorithm are unsatisfactory. First, the way in which the composition of the objectives is formulated in Eq. (5) requires considerable caution to ensure that typical values of $\frac{f_i(\underline{X}_{n+1})}{f_i(\underline{X}_n)}$ are similar for all objectives (otherwise, the search will inevitably favor some objectives over others). Secondly, we have that any movement in which at least one objective is decreased is, potentially, a movement by the search of a non-dominated solution. The probability of acceptance of a movement depends on the relative changes of all objectives (and the temperature of the current system) and, so, there is no guarantee that this movement is going to be accepted. If it isn't, it will not be archived, which is clearly undesirable ((Suppapitnarm *et al.*, 2000)).

In a modification of the original MOSA, Bandyopadhyay *et al.* (2008) found very interesting results in the development of a new formulation: the AMOSA (Archived Multi-Objective Simulated Annealing). The AMOSA algorithm is based on the Simulated Annealing principle. Thus, at a given temperature, T, the probability of a new state s be accepted is equal to:

$$p_{qs} = \frac{1}{1 + e^{\frac{-(E(q,T)) - (E(s,T))}{T}}} \tag{7}$$

The AMOSA incorporates the concept of *archive*, where the non-dominated solutions are stored until then. In this approach, the file size is limited by two boundaries: the hard limit, denominated by HL; and the soft limit, called SL. Another technique used is to group the solutions in the archive, in order to explicitly compel the diversity of non-dominated

solutions ((Bandyopadhyay *et al.*, 2008)).

Other concept used by AMOSA is the amount of domination to calculate the acceptance probability of a new solution. Given two solutions a and b, the amount of domination is defined as $\Delta dom_{a,b} = \prod_{i=1, f_i(a) \neq f_i(b)}^{M} (\|f_i(a) - f_i(b)\| R_i)$, where M is the number of objectives and R_i is the range of the ith objective ((Bandyopadhyay *et al.*, 2008)). This concept can be visualized in Fig. (2).
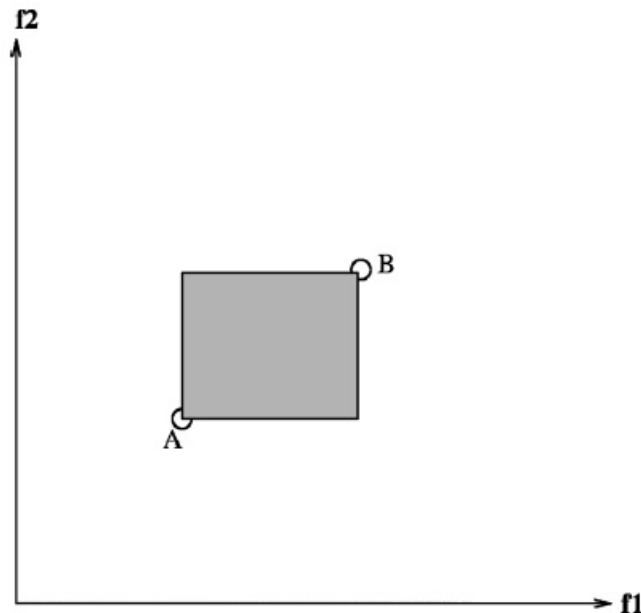
Figure 2: Total Amount of Domination between two solutions A and B = shaded area. Adapted from ((Bandyopadhyay *et al.*, 2008))

6. REGULARIZATION TECHNIQUES

It is known that image reconstruction by EIT generates the formulation of an inverse problem ill-posed. The most common way to address this question is through the regularization of it, using *a priori* information of the object to be studied. In EIT, this information can be anatomical data obtained, for example, by magnetic resonance imaging (MRI), along with known resistivity of different tissues and also the noise level of the measurement system ((Vauhkonen *et al.*, 1998)). Some successful implementations of this information can be found in ((Woo *et al.*, 1992) and (Eyuboglu *et al.*, 1994)). Note, therefore, the importance of choosing the appropriate regularization technique.

6.1 Gradient Norm Method Regularization

6.1.1 Definition

A possible strategy to be used is the development of the regularization function σ_R^{NG} by the Norm of the Gradient Method ((Mojabi and LoVetri, 2009)). This technique penalizes solutions with in benefit of smoother solutions. The formulation of the regularization term is as follows:

$$\sigma_R^{NG} = \int_{\Omega} \|\nabla \sigma\|^2 dA \tag{8}$$

Where Ω is the domain, ∇ denotes the spacial gradient operator and σ is the conductivity distribution.

6.1.2 Application of Norm Gradient Regularization to the TIE Problem

In this case, the multi-objective optimization should be formulated from two objective functions: Eq. (4) and Eq. (8), to be simultaneously minimized.

On a discrete FEM domain, the impedance distribution $\sigma(x)$ is approximated by linear shape functions such that $\sigma(x) = \sigma^T \cdot \Psi(x)$, where σ is the vector of conductivity parameters and $\Psi(x)$ is the vector of base functions. As such, the

A. V. Fernandes, T. C. Martins
Multi-objective optimization by Simulated Annealing Applied to Image Reconstruction by Electrical Impedance Tomography
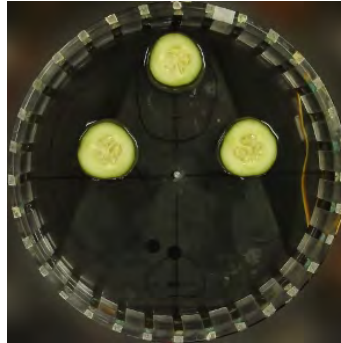
Figure 3: Cucumber phantom that produced the EIT experimental data
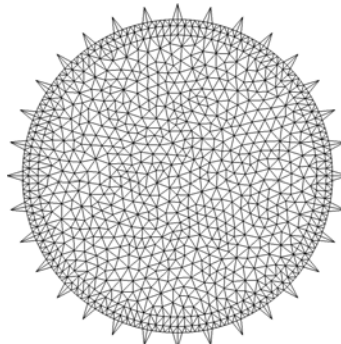
Figure 4: Mesh used for image reconstruction

regularising term σ_R^{NG} can be developed as follows:

$$\sigma_R^{NG} = \int_\Omega \nabla\sigma^2 dA = \int_\Omega \nabla\left(\boldsymbol{\sigma}^T \cdot \Psi\right)^2 dA = \int_\Omega (\boldsymbol{\sigma}^T \cdot \nabla\Psi) \cdot (\nabla\Psi \cdot \boldsymbol{\sigma}^T) dA = \int_\Omega \boldsymbol{\sigma}^T \cdot (\nabla\Psi \otimes \nabla\Psi) \cdot \boldsymbol{\sigma} dA \qquad (9)$$

We can then define by $\mathbf{B}$ the matrix in which:

$$\sigma_R^{NG} = \boldsymbol{\sigma}^T \cdot \mathbf{B} \cdot \boldsymbol{\sigma} \qquad (10)$$

The development of the regularization part depends then of the calculation of the elements b_{ij} of the matrix $\mathbf{B}_{nxn}$, that are, by definition, equal to:

$$b_{ij} = \int_\Omega \nabla\psi_i \nabla\psi_j dA \qquad (11)$$

If the shape functions for the conductivity distribution $\Psi(x)$ are the same used to interpolate the electric potential ϕ, then the $\mathbf{B}_{nxn}$ matrix is very similar to the $\mathbf{K}$ matrix from the FEM model in eq. (3).

7. RESULTS

The experiment in (Martins *et al.*, 2012) was replicated with the cucumber phantom in Figure 3. The FEM mesh - both for impedance and potential discretization - is depicted in Fig. 4. The AMOSA algorithm was implemented with objective functions in Eq. (4) and Eq. (8). It was set to keep at least 15 solutions in the Pareto Front. A graphic representation of the final Pareto Front can be seen in Fig. (5).

The solutions on the Pareto Front can be observed in Fig. (6).

The results of this reconstructions are satisfactory. It can be noticed that this solutions correspond to the higher values of the regularization function (Eq. (8) and, because of this, provide sharper images.
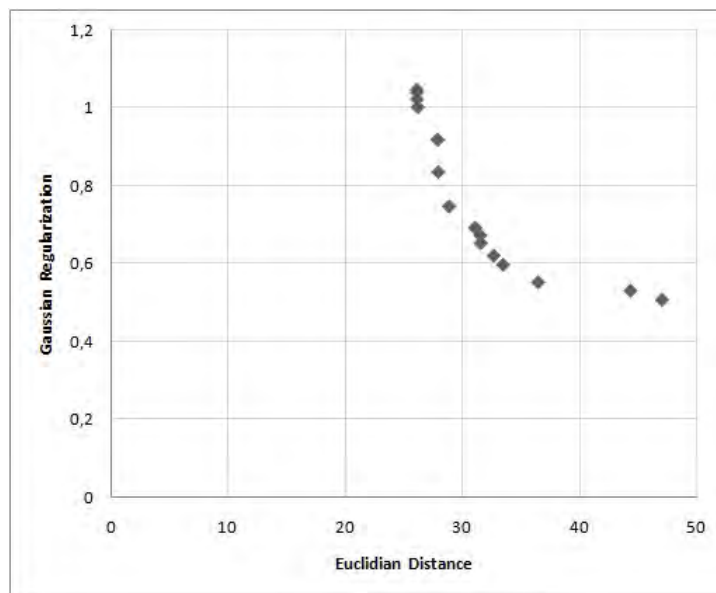
Figure 5: Pareto Front due to the implementation of the bi-objective optimization of the EIT by AMOSA algorithm.

For solutions on the Pareto front, as the value of Eq. (4) increases, the value of Eq. (8) decreases, as it was expected (As all solutions are non-dominating with respect to each other).
The image presents more sharp reconstruction artifacts for lower regularization values. On the other hand, for higher regularization values, the exact position of the cucumber slices become more uncertain.

8. CONCLUSION

In this paper was proposed the use of multi-objective optimization to solve the regularized EIT reconstruction problem, so the appropriate amount of regularization can be selected *after* the reconstruction process is done. An implementation of the AMOSA algorithm, based on Simulated Annealing, was used to perform the multi-objective optimization. Both Euclidean Distance from experimental Data and Norm of the Gradient objective functions were optimized, producing a Pareto front of solutions. As expected, solutions obtained ranged from low regularized, with sharp artifacts to smooth highly regularized solutions, where exact position of the phantom objects is uncertain.

9. ACKNOWLEDGEMENTS

10. REFERENCES

Adler, A. and Guardo, R., 1996. "Electrical impedance tomography: regularized imaging and contrast detection". *Medical Imaging, IEEE Transactions on*, Vol. 15, pp. 170 –179.

Bandyopadhyay, S., Saha, S., Maulik, U. and Deb, K., 2008. "A simulated annealing-based multiobjective optimization algorithm: Amosa". *Evolutionary Computation, IEEE Transactions on*, Vol. 12, pp. 269 –283.

Barber, D.C. and Brown, B.H., 1984. "Applied potential tomography". *Journal of Physics E: Scientific Instruments*, Vol. 17, pp. 723 – 733.

Bates, R.H.T., Garden, K.L. and Peters, T.M., 1983. "Overview of computerized tomography with emphasis on future developments". In *Proceedings of the IEEE*.

Brown, B.H. and Seagar, A., 1987. "The sheffield data collection system". *Clinical Physics and Physiological Measurements*, Vol. 8, pp. A91–A97.

Browne, B.H., 2001. "Medical impedance tomography and process impedance tomography: a brief review". *Measurement Science and Technology*, Vol. 12, p. 991.

Cheney, M., Isaacson, D., Newell, J.C., Simske, S. and Goble, J., 1990. "Noser: An algorithm for solving the inverse conductivity problem". *International Journal of Imaging Systems and Technology*, Vol. 2, pp. 66–75.

Coello, C.A., 2006. "Evolutionary multi-objective optimization: a historical view of the field". *Computational Intelligence Magazine, IEEE*, Vol. 1, pp. 28 – 36.
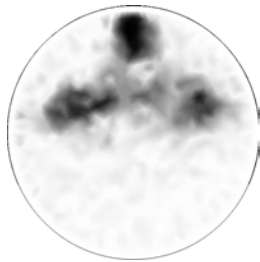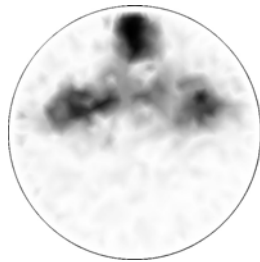
(a) $E(\sigma) = 26.1018$, $\sigma_R^{NG} = 1.04584$ (b) $E(\sigma) = 26.1157$, $\sigma_R^{NG} = 1.0394$ (c) $E(\sigma) = 26.1217$, $\sigma_R^{NG} = 1.02161$
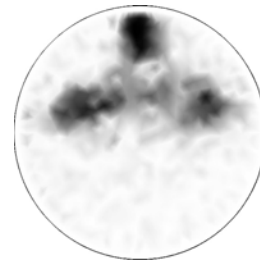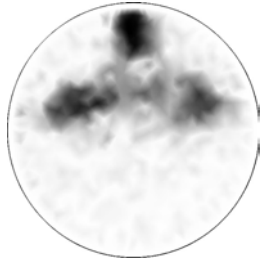
(d) $E(\sigma) = 26.1737$, $\sigma_R^{NG} = 1.00135$ (e) $E(\sigma) = 27.878$, $\sigma_R^{NG} = 0.917577$ (f) $E(\sigma) = 27.9292$, $\sigma_R^{NG} = 0.83473$
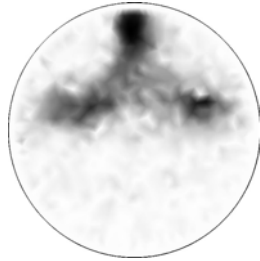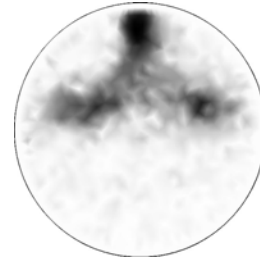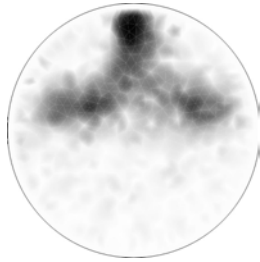
(g) $E(\sigma) = 28.8546$, $\sigma_R^{NG} = 0.74609$ (h) $E(\sigma) = 31.066$, $\sigma_R^{NG} = 0.691234$ (i) $E(\sigma) = 31.5042$, $\sigma_R^{NG} = 0.671725$
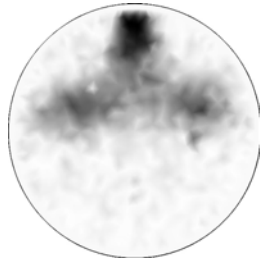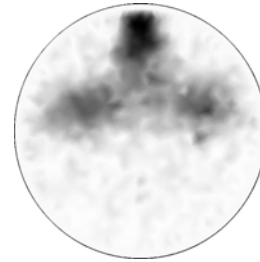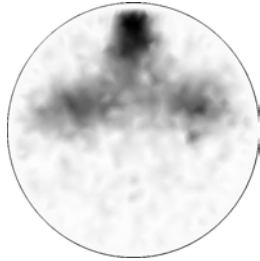
(j) $E(\sigma) = 31.5422$, $\sigma_R^{NG} = 0.55199$ (k) $E(\sigma) = 32.6521$, $\sigma_R^{NG} = 0.6196$ (l) $E(\sigma) = 33.4521$, $\sigma_R^{NG} = 0.595983$
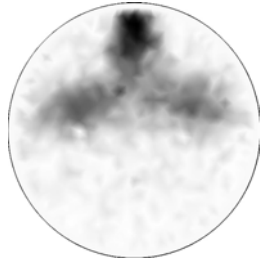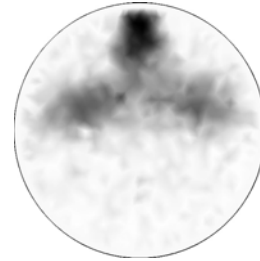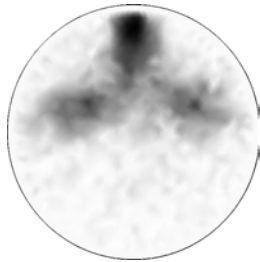
(m) $E(\sigma) = 36.4413$, $\sigma_R^{NG} = 0.55105$ (n) $E(\sigma) = 44.3045$, $\sigma_R^{NG} = 0.529426$ (o) $E(\sigma) = 46.9998$, $\sigma_R^{NG} = 0.506004$
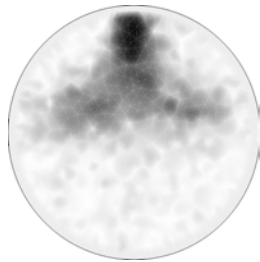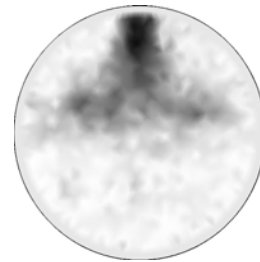
Figure 6: Solutions within the Pareto Front, ordered by increasing $E(\sigma)$

Engrand, P., 1997. "A multi-objective approach based on simulated annealing and its application to nuclear fuel management". In *5th International Conference on Nuclear Engineering*. Nice, France.

Eyuboglu, B.M., Pilkington, T.C. and Wolf, P.D., 1994. "Estimation of tissue resistivities from multiple-electrode impedance measurements". *Physics in Medicine and Biology*, Vol. 39, p. 1.

Frerichs, I., 2000. "Electrical impedance tomography (eit) in applications related to lung and ventilation: a review of experimental and clinical activities". *Physiological Measurement*, Vol. 21, p. R1.

Glisser, D.G., Isaacson, D. and Newell, J.C., 1990. "Electric current computed tomography and eigenvalues". *The Annals of Mathematics*, Vol. 50, pp. 1623–1634.

Henderson, R.P. and Webster, J.G., 1978. "An impedance camera for spatially specific measurements of the thorax". *Biomedical Engineering, IEEE Transactions on*, Vol. BME-25, pp. 250 –254.

Herrera, C.N.L., 2007. *Algoritmo de Tomografia por Impedância Elétrica baseado em Simulated Annealing*. Ph.D. thesis, Escola Politécnica da Universidade de São Paulo, São Paulo, Brazil.

Jones, D.F., Mirrazavi, S.K. and Tamiz, M., 2002. "Multi-objective meta-heuristics: An overview of the current state-of-the-art". *European Journal of Operational Research*, Vol. 137, pp. 1 – 9.

Kallman, J.S. and Berryman, J.G., 1992. "Weighted least-squares criteria for electrical impedance tomography". *Medical Imaging, IEEE Transactions on*, Vol. 11, pp. 284 –292.

Kirkpatrick, S., Jr., C.D.G. and Vecchi, M.P., 1983. "Optimization by simulated annealing". *Science*, Vol. 220, pp. 671–680.

Martins, T., Camargo, E., Lima, R., Amato, M. and Tsuzuki, M., 2012. "Image reconstruction using interval simulated annealing in electrical impedance tomography". *Biomedical Engineering, IEEE Transactions on*, Vol. PP, No. 99, p. 1. ISSN 0018-9294. doi:10.1109/TBME.2012.2188398.

Mello, L.A.M., de Lima, C.R., Amato, M.B.P., Lima, R.G. and Silva, E.C.N., 2008. "Three-dimensional electrical impedance tomography: A topology optimization approach". *Biomedical Engineering, IEEE Transactions on*, Vol. 55, pp. 531 –540.

Mojabi, P. and LoVetri, J., 2009. "Overview and classification of some regularization techniques for the gauss-newton inversion method applied to inverse scattering problems". *Antennas and Propagation, IEEE Transactions on*, Vol. 57, pp. 2658 –2665.

Murai, T. and Kagawa, Y., 1985. "Electrical impedance computed tomography based on a finite element model". *Biomedical Engineering, IEEE Transactions on*, Vol. BME-32, pp. 177 –184.

Ngatchou, P., Zarei, A. and El-Sharkawi, M.A., 2005. "Pareto multi objective optimization". In *Intelligent Systems Application to Power Systems, 2005. Proceedings of the 13th International Conference on*.

Price, L.R., 1979. "Electrical impedance computed tomography (ict): A new ct imaging technique". *Nuclear Science, IEEE Transactions on*, Vol. 26, pp. 250 –254.

Suppapitnarm, A., Seffen, K.A., Parks, G.T. and Clarkson, P.J., 2000. "A simulated annealing algorithm for multiobjective optimization". *Engineering Optimization*, Vol. 33, pp. 59–85.

Sylvester, J. and Uhlmann, G., 1987. "A global uniqueness theorem for an inverse boundary value problem". *The Annals of Mathematics*, Vol. 125, pp. 153–169.

Tikhonov, A.N., 1991. "Ill-posed problems in natural sciences". In *Proceedings of the International Conference*. Moscow, Russia.

Vauhkonen, M., Vadasz, D., Karjalainen, P.A., Somersalo, E. and Kaipio, J.P., 1998. "Tikhonov regularization and prior information in electrical impedance tomography". *Medical Imaging, IEEE Transactions on*, Vol. 17, pp. 285 –293.

West, R.M., Tapp, H.S., Spink, D.M., Bennett, M.A. and Williams, R.A., 2001. "Application-specific optimization of regularization for electrical impedance tomography". *Measurement Science and Technology*, Vol. 12, p. 1050.

Woo, E.J., Hua, P., Webster, J.G. and Tompkins, W.J., 1992. "Measuring lung resistivity using electrical impedance tomography". *Biomedical Engineering, IEEE Transactions on*, Vol. 39, pp. 756 –760.

11. RESPONSIBILITY NOTICE

The authors are the only responsible for the printed material included in this paper.